HK band imaging polarimetry and radiative transfer modeling of CRL 2136

K. Murakawa, T. Preibisch, S. Kraus, and G. Weigelt

Max-Planck-Institut für Radioastronomie, Bonn, Germany

Introduction

CRL 2136 is a massive star-forming region consisting of the near-infrared (NIR) source IRS 1 and a bipolar reflection nebula located at a distance of 2 kpc (Kastner *et al.* 1992). IRS 1 possesses a protostar with a luminosity of $\sim 5\times10^4\,L_\odot$, and its mass was estimated to be higher than $10\,M_\odot$ (Kastner *et al.* 1992). Previous NIR imaging polarimetry (e.g. Minchin *et al.* 1991, Kastner *et al.* 1992) detected two bright lobes of nebulosity extending east and south with respect to IRS 1. Their polarization data shows a centro-symmetrically aligned pattern in the nebulosities surrounding IRS 1 and a linear alignment near IRS 1 with a position angle (PA) of $\sim 45°$. Low resolution spectroscopy has detected deep absorption features of silicate at 9.7 μm ($\tau = 5.07$) and water ice at 3.07 μm ($\tau = 2.72$) (Willner *et al.* 1982). A CO emission line map shows blue- and red-shifted outflow components extending toward the southeast ($\sim 135°$) and the northwest ($\sim -45°$), respectively, approximately perpendicular to the direction of aligned polarization vectors near the central star (Kastner *et al.* 1994). The above-mentioned observational results are strong evidence for an optically thick torus, a possibly disk, and an envelope structure.

In recent years, some observational insights into the circumstellar environment of massive protostars have been obtained through high-resolution NIR imaging (e.g. Weigelt *et al.* 2006) and radio interferometry (e.g. Patel *et al.* 2005, Steinacker *et al.* 2006). Furthermore, the circumstellar environment of young stellar objects (YSOs) is also known to be a molecular-forming region. Various absorption features, such as water ice, formaldehyde, and methanol, have been detected in the circumstellar environment (e.g. van Dishoeck *et al.* 2004, Gibb *et al.* 2004). These molecules are thought to form on dust grains, which work as a catalyst to promote chemical reactions (e.g. Jones & Williams 1984). The chemical reactions (or molecular formation) depend on physical conditions such as the dust temperature and the dust and gas densities. Therefore, investigating the physical properties of the dusty environment around young stellar objects is important in order to obtain a better understanding of the formation of massive stars as well as the chemical evolution in their surroundings.

Observations

Near-infrared imaging polarimetry is a powerful technique to extract important information of dust shell structures which is hard to detect from the total intensity images (e.g. Murakawa *et al.* 2008a). We obtained the *H* and *K*-band polarimetric images of CRL 2136 using the near-infrared camera CIAO on the 8 m Subaru telescope on June 28, 2005. A turnable half-wave plate and a wire-grid polarizer allowed us to measure linear polarization. The Stokes *IQU* parameter images, the degree of linear polarization images, and the polarization orientation were derived from the observed data (Fig. 1 middle and bottom; see also the top-left sketch of CRL 2136).

Our images show:

- The bright infrared source IRS 1 and fan-shaped nebulisities extending towards the south, east, west, and northwest.
- In the nebulosities, the polarization vectors are centro-symmetrically aligned and the polarization reaches $P_H = 30\,\%$ and $P_K = 50\,\%$.
- At IRS 1, the polarization vectors are systematically aligned along the polarization disk, which is spatially resolved in our data. In this region, the polarization is enhanced at a spot-like shape and is as high as $P_H = 32\,\%$ and $P_K = 21\,\%$.
- A fan-shaped region with low polarizations between the southern and eastern lobes and IRS 1. This region is probably the projected inner part of the envelope cavity.

Radiative transfer modeling

We have performed two-dimensional radiative transfer calculations to model the disk and infalling envelope of CRL 2136. We constrain the model parameters by fitting the spectral energy distribution (SED), the total intensity images, and the polarization images.

We used our own Monte Carlo radiative transfer code (**STSH**), which:

- simulates scattering and thermal emission of radiation by spherical dust grains in a three-dimensional model geometry.
- can treat multiple grain models.
- allows a proper treatment of polarized light (Fischer *et al.* 1994)
- uses techniques to improve the Monte Carlo noise in the resulting images (e.g. Witt 1977, Yusef-Zadeh *et al.* 1984).
- computes the SEDs, the dust temperature, and the Stokes *IQUV* images.

We applied model geometries with a disk and infalling envelope, given by $\rho = \rho_{\rm disk} + \rho_{\rm env}$. For the disk structure, a Keplerian rotating disk is often used. However, we find that Toomre's model (Toomre 1982) fits better in the SED. For the envelope, we use the model of the slowly rotating, infalling envelope (Ulrich 1976, Cassen & Moosman 1981, Terebey 1984). These forms are given with the two-dimensional cylindrical coordinate (r, z) and $R = \sqrt{r^2 + z^2}$ by

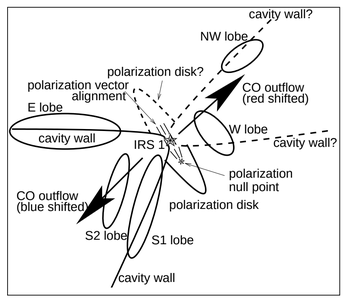

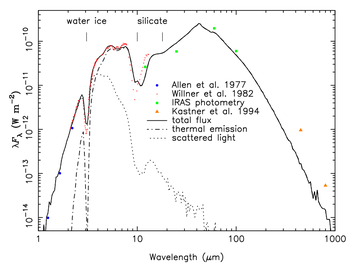

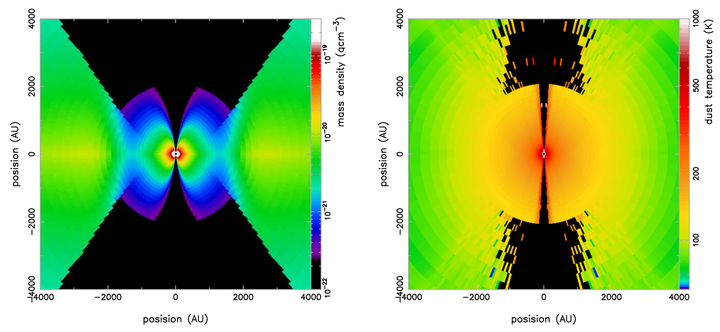

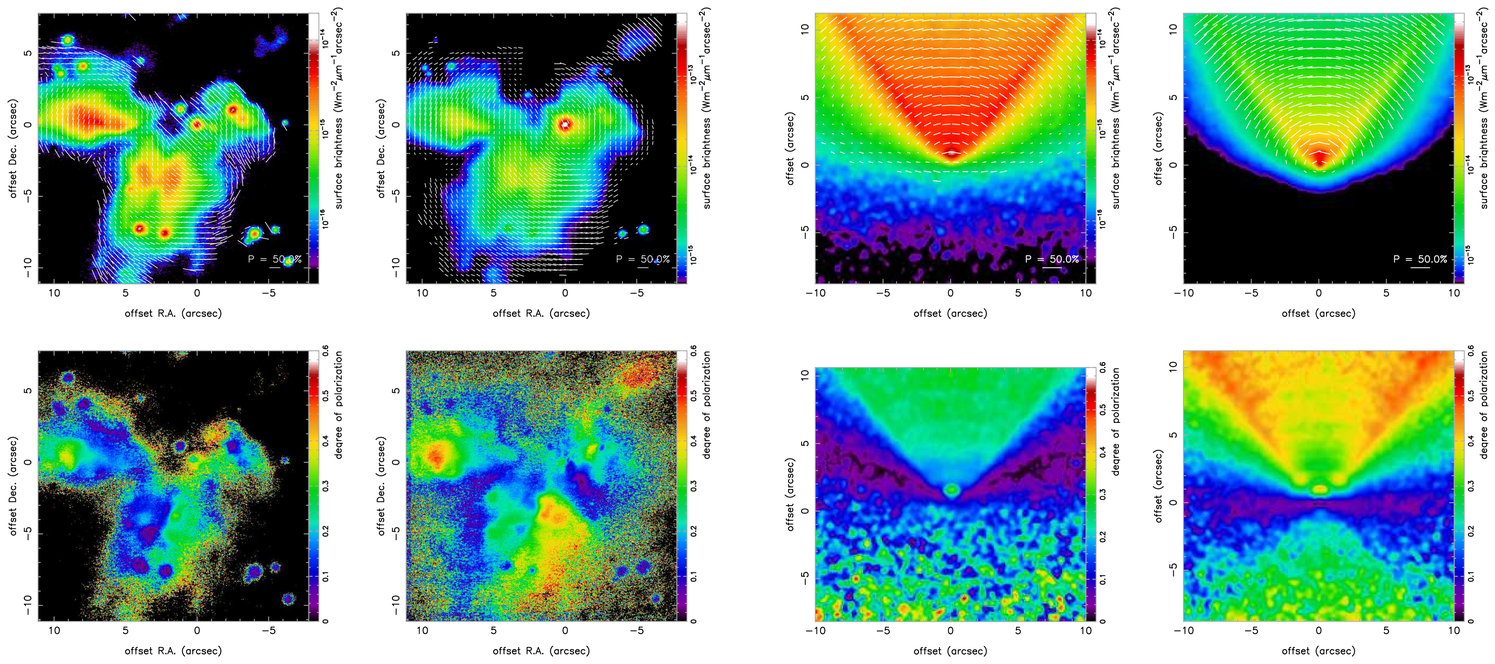

Figure 1: *top-left*: Cartoon of CRL 2136 illustrating the features detected in our data, the direction of the CO outflow, as well as our interpretation of a disk and envelope structure. *middle & bottom*: The intensity images with polarization vector lines and the degree of polarization images. The left and right panels are in the *H* and *K* bands, respectively. *top-right*: Comparison of the model SED to observations.

Figure 2: The results of our radiative transfer modeling. *top*: The mass density distribution (*left*) and the dust temperature distribution (*right*). *middle & bottom*: intensity images with polarization vector lines and the degree of polarization images. The left and right panels are in the *H* and *K* bands, respectively.

$$\rho_{\rm disk}(r,z) = \rho_{\rm d}\,(r/R_{\rm disk})^{-2}\exp\left(-\left|\frac{z}{Hr}\right|\right),$$

$$\rho_{\rm env}(R,\mu) = \frac{\dot{M}_{\rm env}}{4\pi\sqrt{GM_\star R^3}}\left(1+\frac{\mu}{\mu_0}\right)^{-1/2}\left(\frac{\mu}{\mu_0}+\frac{2\mu_0^2 R_{\rm c}}{R}\right)^{-1},$$

where $R_{\rm disk}$ and H are the disk radius and the disk scale height, respectively. The quantity $\rho_{\rm d}$ is determined by the disk mass $M_{\rm disk}$. For the disk parameter, we set an inner radius $R_{\rm in}$ of 30 AU, a dust sublimation radius. Thus, the free parameters are $M_{\rm disk}$, $R_{\rm disk}$, and H. For the envelope parameters, we set the stellar mass $M_\star$, the centrifugal radius $R_{\rm c}$, and the angle of a stream line μ_0 to be $20\,M_\odot$, $R_{\rm disk}$, and $\cos(65°/2)$, respectively. The free parameters are the mass infalling rate $\dot{M}_{\rm env}$ and the outer radius $R_{\rm out}$.

We apply three dust components: (1) bare grains at the dust temperature between 140 K and 1500 K, (2) warm grains with a crystalline water ice mantle at 80 K $\lesssim T_{\rm d} \lesssim$ 140 K, and (3) cold grains with an amorphous water ice mantle at $T_{\rm d} \lesssim 80$ K. We assume an MRN-like size distribution; i.e., $0.005\,\mu{\rm m} \le a \le a_{\rm max}$ and $n(a) \propto a^{-3.5}$. The $a_{\rm max}$ is determined to be 0.45 μm using a one-dimensional single scattering model (Dougados *et al.* 1990). We do not find evidence for the presence of larger grains.

Other parameters are determined by fitting the SED, intensity images, and polarization images. The parameter values are summarized in Table 1, and the model results are presented in Fig. 1 (top-right) and 2.

Parameters	Values	Range
stellar parameters		
effective temperature ($T_{\rm eff}$)	20,000 K	adopted
luminosity ($L_\star$)	55,000 $L_\odot$	Kastner *et al.* 1992
stellar mass ($M_\star$)	20 $M_\odot$	Bernasconi & Maeder 1996
distance	2 kpc	Kastner *et al.* 1992
dust grains		
size ($a_{\rm max}$)	0.45 μm	0.4 – 0.5
grain core	DL-chemistry	Draine & Lee 1984
warm ice mantle	crystalline H_2O	Bertie *et al.* 1969
cold ice	amorphous H_2O	Leger *et al.* 1983
disk		
inner radius ($R_{\rm in}$)	30 AU	adopted
disk radius ($R_{\rm disk}$)	2000 AU	2000 – 3000
disk mass ($M_{\rm disk}$)	0.007 $M_\odot$	0.007 – 0.01
scale height (H)	1	1 – 2
accretion rate ($\dot{M}_{\rm acc}$)	$2.1\times10^{-7} M_\odot{\rm yr}^{-1}$	calculated
infalling envelope		
infalling rate ($\dot{M}_{\rm env}$)	$1.0\times10^{-4} M_\odot{\rm yr}^{-1}$	1.0 – 1.5×10^{-4}
outer radius ($R_{\rm out}$)	0.5 pc	0.3 – 0.5
μ_0	$\cos(65°/2)$	estimated
envelope mass ($M_{\rm env}$)	177 $M_\odot$	calculated

Table 1: Parameters of our two-dimensional radiative transfer modeling.

Implications

- The CRL 2136 disk has a large radius (2000 AU), a low mass (0.007 $M_\odot$), and a puffed-up structure (H=1). The central star with 20 $M_\odot$ formed rapidly ($\sim 2\times10^5$ yr) with a high infalling rate and nearly isotropically in the beginning of the star formation process. Then, after ignition of the central star, the string radiation pressure from the luminous central star halted the accretion of the disk matter.
- Because of this disk structure, the dust is efficiently heated by the central star ($T_{\rm d} \gtrsim 100$ K). The disk is optically thin for photons at $\lambda = 3.08\,\mu$m, and H_2O molecules responsible for the 3 μm absorption feature mainly exist in the inner part of the envelope rather than in the disk.
- The polarization vector alignment towards IRS 1 is produced by dichroic absorption by sub-micron-sized, non-spherical grains because (1) the disk is not expected to have a geometrically thin structure, which is thought to produce polarization vector alignment (Bastien & Ménard 1988), (2) the region of enhanced polarization towards IRS 1 has a spot shape, and (3) the polarization is not reproduced by our modeling, which convolves the equivalent PSF to the observations.

References

Allen, D. A., Hyland, A. R., Longmore, A. J., *et al.* 1977, *A&A* **217**, 108
Weigelt, G., *et al.* 2006, *A&A* **447**, 655
Bastien, P., & Ménard, F. 1988, *ApJ.* **326**, 334
Bertie, J. E., *et al.* 1969, *J. Chem. Phys.* **50**, 4501
Bernasconi, P. A., & Maeder, A. 1996, *A&A* **307**, 829
Cassen, P., & Moosman, A. 1981, *Icarus* **48**, 353
Dougados, C., Rouan, D., Lacombe, F., Forveille, T., & Tiphene, D. 1990, *A&A* **227**, 437
Draine, B. T. & Lee, H. M. 1984, *ApJ.* **258**, 89
Fischer, O., Henning, Th., & Yorke, H. W. 1994, *A&A* **284**, 187
Gibb, E. L., Whittet, D. C. B., Boogert, A. C. A., & Tielens, A. G. G. M. 2004, *Astrophys. J.-Suppl. Ser.* **151**, 35
Jones, A. P., & Williams, D. A. 1984, *MNRAS* **209**, 955
Kastner, J. H., Weintraub, D. A., & Aspin, C. 1992, *ApJ.* **389**, 357
Kastner, J. H., Weintraub, D. A., Snell, R. et al. 1994, *ApJ.* **425**, 695
Leger, A., Gauthier, S., Defourneau, D., & Rouan, D. 1983, *A&A* **117**, 164
Minchin, N. R., Hough, J. H., Burton, M. G., & Yamashita, T. 1991, *MNRAS* **251**, 522
Murakawa, K., Ohnaka, K., Driebe, T. et al. 2008a, *A&A* , in press
Murakawa, K., Preibisch, T., Kraus, S., et al. 2008b, *A&A* **488**, L75
Murakawa, K., et al. 2008c, *A&A* , submitted
Patel, N. A., Salvador, C., Sridharan, T. K., *et al.* 2005, *Nature* **437**, 109
Steinacker, J., Chini, R., Nielbock, M., *et al.* 2006, *A&A* **456**, 1013
Terebey, S., Shu, F. H., & Cassen, P. 1984, *ApJ.* **286**, 529
Toomre, A. 1982, *ApJ.* **259**, 535
Ulrich, R. K. 1976, *ApJ.* **210**, 377
van Dishoeck, E. F. 2004, *Ann. Rev. Astron. Astrophys.* **42**, 119
Willner, S. P., Gillett, F. C., Herter, T. L., Jones, B., *et al.* 1982, *ApJ.* **253**, 174
Witt, A. N. 1977, *Astrophys. J.-Suppl. Ser.* **35**, 1
Yusef-Zadeh, F. Morris, M., & White, R. K. 1984, *ApJ.* **278**, 186

Murakawa, K., Preibisch, T., Kraus, S., & Weigelt, G. 2008, *A&A* , in press
Poster presented at Cosmic Dust Near & Far 2008
8th-12th September 2008, Heidelberg, Germany
contact e-mail: murakawa@mpifr-bonn.mpg.de